**ABUAD Journal of Engineering Research and Development (AJERD)**
**ISSN (online): 2645-2685; ISSN (print): 2756-6811**

Volume 8, Issue 2, 268-283

# Performance Assessment of Organic Fibre-Reinforced Ceiling Boards for Sustainable Building Applications

Theophilus Olukunle OLOYEDE[1,2], Joseph ABUTU[2], Zaka Audu MSHELIA[3]

[1]*Advanced Manufacturing Technology Development Institute, Jalingo-Nigeria*
theotimothy@gmail.com

[2]*Department of Mechanical Engineering, Taraba State University, Jalingo, Nigeria*
abutu.joseph@tsuuniversity.edu.ng

[3]*Department of Mechanical Engineering, University of Maiduguri, Maiduguri-Nigeria*
mshelia968@gmail.com

*Corresponding Author:* abutu.joseph@tsuuniversity.edu.ng, +2347035241729
*Date Submitted:* 10/06/2025
*Date Accepted:* 12/07/2025
*Date Published:* 03/08/2025

***Abstract:*** *This study developed two separate ceiling boards using snot apple fibre and cow hair with coconut shells and epoxy resin binder added in each of the boards in order to produce sustainable, lightweight, and cost-effective ceiling boards from agricultural and animal waste fibres as eco-friendly alternatives to conventional, non-renewable building materials. Natural fibres from plant and animal wastes were treated with sodium hydroxide and characterized by X-ray fluorescence, revealing distinct elemental compositions: coconut shell fibre rich in MgO (33.318%) and $SiO_2$ (20.044%), cow hair fibre high in $SO_3$ (54.35%), and snot apple fibre rich in MgO (38.006%) and $SiO_2$ (21.409%). Composite samples were produced via compression moulding using a Taguchi L9(3)3 design to vary filler, additive, and binder content systematically. Mechanical properties (tensile strength, hardness, impact energy), water absorption, thickness swelling, and microstructure were evaluated. Snot apple fibre-based boards (SAF) showed superior tensile strength (12.51MPa), hardness (79.5HVN), and impact energy compared to cow hair fibre boards (CHF) shows 9.29MPa tensile strength, 73.3HVN hardness, though with greater variability and thickness swelling. ANOVA revealed filler content primarily influenced cow hair boards' tensile strength and hardness, while coconut shell and binder content were key for snot apple boards. Epoxy resin significantly affected water absorption and swelling in both, necessitating tailored formulations. SEM analysis performed on the optimised samples confirmed microstructural features correlating with performance while thermogravimetric analysis revealed that SAF ceiling boards demonstrates significantly superior thermal stability compared to the CHF composite, making it more suitable for high-temperature applications. Overall, the composites are suitable eco-friendly alternatives for ceiling board applications in building.*

***Keywords:*** *Snot Apple Fibre, Cow Hair, Coconut Nut Shells, Epoxy Resin, Ceiling Boards, Taguchi*

## 1. INTRODUCTION

The construction industry is increasingly prioritizing the development of innovative materials that effectively combine high performance, environmental sustainability, and cost-efficiency. While traditional building materials such as steel, concrete, and asbestos-cement have long been favoured for their strength and durability, they come with significant disadvantages. These include their considerable weight, substantial environmental footprint due to energy-intensive production processes, and, in the case of asbestos-cement, serious health risks associated with asbestos exposure [1-2]. In light of these challenges, there has been a growing surge in research focused on composite materials, especially those reinforced with natural fibres derived from renewable and organic waste sources [3-4]. Natural fibre composites (NFCs) are rapidly gaining traction within the construction sector because they offer a range of benefits, including environmental friendliness, biodegradability, affordability, and competitive mechanical properties [5]. These fibres, which originate from both plant and animal sources such as coconut shells, cow hair, and snot apple fibres are often abundant by-products of agricultural and industrial activities. When left unutilized, these materials contribute significantly to environmental pollution and waste management problems. By integrating these natural fibres into composite matrices, manufacturers not only add value to what would otherwise be discarded as waste but also provide a sustainable and renewable alternative to conventional, non-renewable construction materials.

Moreover, the use of natural fibre composites aligns with global efforts to promote circular economy principles by transforming agricultural residues and industrial by-products into high-performance building materials [21-22]. This approach reduces reliance on finite resources, lowers carbon emissions associated with material production, and mitigates waste accumulation in landfills. Additionally, natural fibre composites often exhibit favourable properties such as lightweight structure, good thermal and acoustic insulation, and adequate mechanical strength, making them suitable for a

wide range of construction applications including ceiling boards, wall panels, and insulation materials. As research continues to optimize the processing techniques and material formulations, natural fibre composites are poised to become a cornerstone of sustainable construction, offering eco-friendly solutions that meet both performance standards and economic considerations [23]. Also, ceiling boards, as essential interior building components, has become a focal point for sustainable material innovation [6-7]. The demand for lightweight, durable, and moisture-resistant ceiling panels has driven research towards green composites that utilize organic waste materials. These bio-based composites offer the potential to reduce greenhouse gas emissions, lower carbon footprints, and minimize the environmental and health risks associated with traditional ceiling materials [8]. Despite their advantages, natural fibre composites face challenges such as variability in fibre properties, extensive treatment to improve compatibility with polymer matrices, and the need for optimized processing techniques to achieve consistent performance. Recent advancements in material science and design methodologies, including the use of statistical optimization techniques like the Taguchi method, have enabled the development of high-performance organic fibre-reinforced composites tailored for construction applications.

Several works have been carried out using natural wastes for production of composite such as particle boards and ceiling boards; Oladele et al. [9] investigated natural fibre-reinforced polymer composites using agricultural wastes (palm kernel shell fibre/particulate cassava peel) and found that natural fibres are lightweight, biodegradable, and cost-effective but face challenges like poor interfacial adhesion and moisture sensitivity. Hence, the authors recommended that fibre should be pre-treated to improve surface properties and reduce moisture absorption, enhancing composite performance. Also, Abutu et al. [10] investigated agro-based particle boards made from sugarcane bagasse and rice husk as fillers, combined with low-density polyethylene (LDPE) and coconut shell. The authors reported that the organic waste materials, particularly sugarcane bagasse, offer viable alternatives for sustainable particleboard production. In addition, Ameh et al. [11] investigated the production of ceiling boards using rice husk and cassava starch. The ceiling boards were produced by mixing rice husk and cassava starch in ratios from 70:30 to 30:70 with epoxy resin. The authors found that increasing cassava starch concentration in ceiling boards raised density overall but caused non-linear effects on other properties: flaking decreased up to 40wt% starch, rebounded above this threshold, then declined again beyond 50wt%; water absorption generally increased with starch content but temporarily dropped at 60wt% before rising further. The work of Guredam and Ossia [4] found that green composites made from organic wastes like groundnut shells and sawdust reduce greenhouse gas emissions while offering mechanical properties comparable to conventional materials, with Zeleke's banana fibre-reinforced polyvinyl-acetate boards demonstrating lightweight, biodegradable panels featuring competitive thermal conductivity ($9.2 \times 10^{-2}$ W/mK) and water absorption (8.6%). Also, Ezenwa et al. [12] produced boards from breadfruit seed coat and recycled LDPE, and found that that composites with 40% filler content achieved a flexural strength of 19.32 MPa, comparable to commercial boards, demonstrating the viability of agro-waste for reducing environmental pollution.

Additionally, the work of Jeremiah Lekwuwa et al. [13] focused on the production and thermo-structural analysis of a hybridized natural fibre-based ceiling board intended for building applications using local agricultural wastes (Canewood and palm kernel fibre with recycled low-density polyethylene (LDPE) as the binder. The authors found that cane wood and palm kernel fibre fillers demonstrated thermal stability up to 325°C and 310°C, respectively; the optimized ceiling board containing 15% cane wood, 10% PKF, and 75% LDPE showed excellent performance confirming the suitability of LDPE-based fillers for ceiling board applications. Also, Ikubanni et al. [14] investigated particleboards made from waste ceramics, waste paper, and sawdust bonded with urea formaldehyde. Finding showed that the boards met key physical and mechanical standards with densities of 761.9–1142 kg/m³, acceptable water absorption and thickness swelling, and suitable modulus of elasticity and rupture for structural and interior use, recommending a 20% increase in adhesive to enhance properties. Therefore, this study aims to develop and characterize two different ceiling boards reinforced with locally sourced organic wastes-specifically cow hair, and snot apple fibres while coconut shells and epoxy resin matrix were used in each of the board as additive and binder respectively. By evaluating the performance, microstructure and thermal stability of these green composites, this research seeks to demonstrate the viability of organic waste-based ceiling boards as sustainable alternatives for the building industry.

## 2. MATERIALS AND METHODS

### 2.1 Materials

Materials used for this research include; Coconut shells (Figure 1a) sourced from a coconut trader in Jalingo market. Jalingo-Nigeria, cow hair (Figure 1b) obtained from cow sellers at Abattoir market, Jalingo-Nigeria and snot apple fibre (Figure 1c) sourced from an open market in the Tula area of Kaltungo Local Government Area, Gombe State-Nigeria where it was available in commercial quantity. Also, epoxy resin (Commercial grade) along with epoxy hardener a medium-viscosity epoxy curing agent was purchased from a chemical store in Lagos-Nigeria.

In addition, the mould used for the production of the samples was fabricated using mild steel sheet plate with dimension of 120 x 180 x 3 mm while Hardness testing was performed using a Vicker Hardness Tester (Model: MV1-PC, Serial No.: 07/2012-1329); Impact testing utilized a Cat.Nr.412 Charpy Test Machine (S/No: 412-07-15269C). Also, tensile strength was measured with a Universal Testing Machine (Instron Series 3369) while water absorption was assessed using an Electronic Compact Scale; X-ray fluorescence (XRF) analysis was conducted with a using Xenemetrix Genius IF benchtop Energy Dispersive X-ray Fluorescence (EDXRF) spectrometer and microstructure of developed samples were assessed with scanning electron microscopy was carried out equipped with Energy Dispersive X-ray Spectroscopy (SEM-EDX).

(a) (b) (c)

Figure 1: Production materials (a) Coconut shells (b) Cow hair (c) Snot apples

## 2.2 Methods

### 2.2.1 Material Preparation

Coconut shell collected were washed, treated with sodium hydroxide (NaOH) solution, sun-dried for 5 days to remove moisture, crushed with mortar and pestle, ground using a grinding machine, and sieved to 125 µm. Also, snot apple fibres were prepared by soaking the chewed apple fibres in NaOH solution, sun-dried for 5 days, and cut into 40 mm lengths. In addition, cow hair fibres were obtained by scraping hairs from white cow tails, thoroughly washed, treated with NaOH, sun-dried for 5 days, and cut into 10 mm lengths.

### 2.2.2 Characterization of prepared materials

The prepared cow hair fibre, snot apple fibre, and coconut shell powder samples were characterised using X-ray fluorescence in order to determine their elemental composition and assess their suitability for use as ceiling board in building material applications. The procedure adopted for the X-ray fluorescence (XRF) experiment was in accordance with ASTM D6247 which involved irradiation of the sample with high-energy X-rays that eject inner shell electrons; as electrons from higher orbitals fill these vacancies, characteristic fluorescent X-rays are emitted and detected by an energy-dispersive detector like a Silicon Drift Detector (SDD) to produce a spectrum for qualitative and quantitative elemental analysis.

### 2.2.3 Taguchi experimental design

Experimental design was carried out in accordance with standard Taguchi's $L_9(3)^3$. Nine sets each of Snot Apple Fibre reinforced (SAF) and Cow Hair Reinforced (CHF) composite samples with varying compositions were produced in order to determine the optimum level of ingredients. Cow hair and snot apple fibres are used separately as based fibre reinforced fibres while Coconut shells and epoxy resin as additives and binder respectively. However, constant process parameters (moulding time-10minutes, moulding temperature-130˚C, moulding pressure-100MPa and heat treatment time-1hour) adopted by Abutu, et al. [15] were utilised during the production. Table 3.1 shows the three factors at three levels while Table 3.2 show the Taguchi orthogonal arrays and experimental design matrix.

Table 1: Factor levels for variables employed in the Taguchi design.

| **Factors** | **Level 1 ($L_1$)** | **Level 2 ($L_2$)** | **Level 3 ($L_3$)** |
|---|---|---|---|
| Filler (g) | 50 | 60 | 70 |
| Additive (g) | 80 | 90 | 100 |
| Binder (g) | 100 | 110 | 120 |

Table 2: Taguchi's $L_9(3)^3$ experimental design matrix

| | Orthogonal array | | | Experimental matrix | | |
|---|---|---|---|---|---|---|
| *Run* | Filler (g) | Additive (g) | Binder (g) | Filler (g) | Additive (g) | Binder (g) |
| 1 | 1 | 1 | 1 | 50 | 80 | 100 |
| 2 | 1 | 2 | 2 | 50 | 90 | 110 |
| 3 | 1 | 3 | 3 | 50 | 100 | 120 |
| 4 | 2 | 1 | 2 | 60 | 80 | 110 |
| 5 | 2 | 2 | 2 | 60 | 90 | 120 |
| 6 | 2 | 3 | 1 | 60 | 100 | 100 |
| 7 | 3 | 1 | 3 | 70 | 80 | 120 |
| 8 | 3 | 2 | 1 | 70 | 90 | 100 |
| 9 | 3 | 3 | 2 | 70 | 100 | 110 |

### 2.2.4 Production of ceiling board samples

Sample production was carried out using compression moulding machine (Model: 0577-86365889, Wenzhou Zhiguang Shoe Machine Co. Ltd) situated at Nigerian Institute for Leather and Science Technology (NILEST), Samaru, Zaria-Nigeria. The weights of filler fibres (cow hair and snot apple fibres), additives (coconut shell powder), and epoxy resin were measured using an electronic compact scale as detailed in Table 2. Process parameters were kept constant throughout moulding, while composition varied according to the experimental design. A release agent was applied to aluminum foil lining the mould to facilitate easy removal after curing. Following Abutu et al. [15], epoxy resin was mixed with hardener in a 2:1 ratio, then combined with the pre-mixed filler fibres and additives. The mixture was thoroughly stirred with a metallic stirrer to ensure homogeneity. The blend was poured into the mould and cured in a compression moulding machine at 130°C, 100 MPa pressure, for 10 minutes. After moulding, samples were removed and further cured in a hot air oven at 150°C for 1 hour. This procedure was consistently applied to all samples to achieve optimal properties.

The developed cow hair fibre based ceiling boards (CHF) and snot apple fibre based ceiling boards (SAF) samples obtained from compression moulding is shown in Figure 2(a) and Figure 2(b) respectively.


(a) (b)

Figure 2: Developed ceiling board samples (a) CHF (b) SAF

### 2.2.4 Sample characterisation

Developed ceiling board samples were characterised to assess the mechanical (tensile strength, hardness and impact energy), physical (water absorption and thickness swelling) and morphological (microstructure) properties. The tensile test was conducted in accordance with ASTM D638 using an electronic universal testing machine (Instron 3369), which measured properties such as modulus of elasticity, elastic limit, elongation, tensile strength, and yield strength by applying a gradually increasing tensile load until the specimen breaks, recording the corresponding extension. Also, the hardness test follows ASTM D2240 (Type D scale) standard using a Vicker Hardness Tester with a 0.3 kgf load and 10-second dwell time at three points, automatically reading hardness values while Impact was obtained by ASTM E23 using a Charpy impact tester on notched specimens (80×10×10 mm) with a 45° notch, measuring the energy absorbed upon impact.

In addition, water absorption of the developed samples was assessed using ASTM D570 standard for 72 hours by weighing dried specimens before and after 24-hour immersion in distilled water to calculate weight change and percentage absorption (Equation 1), and thickness swelling, measured by marking specimens at three points, periodically measuring thickness changes after water immersion, and calculating percentage swelling from initial and swollen thickness values using Equation 2. Also, the microstructure of tensile fracture specimen obtained from tensile test was assessed at X100 magnification using a scanning electron microscope

$$\text{Percentage water absorption by weight after 24 hours} = \frac{\Delta W}{W1} \times 100 \quad (1)$$

$$\text{Percentage Thickness Swell (\%T)} = \frac{\Delta T}{T1} \times 100 \quad (2)$$

Where;

$\Delta W$ = Weight loss after 24 hours = Final weight ($W_2$) – Initial weight ($W_1$)

$\Delta T$ = Change in thickness after 24 hours = Swollen Thickness ($T_2$) – Initial Thickness ($T_1$)

### 2.2.6 Microstructural and thermal characterization

i. **Scanning Electron Microscopy (SEM-EDX):** The impact-fractured surfaces of optimized CHF and SAF samples were examined using a scanning electron microscope equipped with Energy Dispersive X-ray Spectroscopy (SEM-EDX). Prior to analysis, samples were sputter-coated with a thin gold layer to enhance electrical conductivity. Observations were conducted at an accelerating voltage of 10 kV. Specimens were mounted on the microscope stage, and fine adjustments to focus and alignment were made using control knobs to optimize image clarity. High-resolution

micrographs were captured digitally at the desired magnification using integrated software and archived for further analysis.

ii. **Thermogravimetric Analysis (TGA):** Thermal stability of optimized CHF and SAF samples was evaluated using a Perkin Elmer Pyris TGA 1 analyzer (USA). Approximately 16 mg of each sample was loaded into platinum pans and heated from 30°C to 900°C at a rate of 10.00°C/min under a nitrogen atmosphere with a flow rate of 20 mL/min. Weight changes during heating were monitored and analyzed via Pyris software. The peak degradation temperature (($T_p$) defined as the temperature at which maximum material decomposition occurred was determined from the derivative thermogravimetric (DTG) curve, representing the peak of the derivative weight loss over time.

## .3. RESULTS AND DISCUSSION

### 3.1 X-Ray Fluorescence

The elemental composition of the prepared materials used in this study, obtained from X-ray fluorescence (XRF) analysis, is presented in Table 3. The XRF analysis indicates that coconut shell is dominated by magnesium oxide (MgO: 33.318%), silicon dioxide ($SiO_2$: 20.044%), calcium oxide (CaO: 10.072%), and chlorine (Cl: 13.902%), with significant amounts of alumina ($Al_2O_3$: 7.759%) and potassium oxide ($K_2O$: 7.057%), alongside minor impurities (e.g., $SO_3$: 2.669%, $P_2O_5$: 0.736%) and trace elements (<1%). The material's magnesium silicate-like structure (MgO + $SiO_2$ > 53%) and unusual chlorine content suggest parallels to industrial ceramics or chloride-rich matrices, while low transition metals ($Fe_2O_3$: 2.55%, CuO: 0.75%) and the absence of $SnO_2$ reflect environmental influences and elemental purity. Additionally, the XRF results for cow hair fibres revealed a sulfate-dominated material ($SO_3$: 54.35%) paired with calcium oxide (CaO: 18.81%), strongly suggesting that cow hair fibre is a sulfate-rich industrial by-product, with minor silicates ($SiO_2$: 13.36%), trace metals (e.g., CuO: 0.248%, ZnO: 0.394%), and notable chlorine (Cl: 6.88%) likely from environmental or processing-related contamination, while the absence of MgO and BaO indicates elemental purity in the cow hair fibres.

Furthermore, the XRF results for snot apple fibre revealed a magnesium-rich material (MgO: 38.006%) with significant silicon dioxide ($SiO_2$: 21.409%) and calcium oxide (CaO: 18.129%), suggesting a magnesium silicate-based composition, alongside minor impurities ($SO_3$: 5.745%, Cl: 7.396%), trace metals (CuO: 0.297%, ZnO: 0.222%), and purity in certain elements (such as the absence of $SnO_2$ and minimal $Ag_2O$: 0.003%). The magnesium oxide, silicon dioxide, and calcium oxide in the coconut shells and snot apple fibre signify strong potential for refractory and ceramic applications with notable chemical durability. Cow hair fibre, dominated by sulfate, calcium oxide, and silicon dioxide, appears to be a sulfate-rich industrial by-product offering fire retardancy and high elemental purity. Generally, the presence of MgO and $SiO_2$ in cow hair, coconut shell, and snot apple fibres provides mechanical reinforcement and thermal stability, making them suitable as eco-friendly, lightweight, and durable materials for ceiling board applications.

Table 3: Elemental composition of prepared materials

| S/N | Component | Mole % | | |
|---|---|---|---|---|
| | | Coconut shell | Cow Hair Fibre | Snot apple fibre |
| 1 | $SiO_2$ | 20.044 | 13.360 | 21.409 |
| 2 | $Fe_2O_3$ | 2.551 | 0.321 | 0.285 |
| 3 | $CO_3O_4$ | 0.30 | 0.004 | 0.003 |
| 4 | CuO | 0.750 | 0.248 | 0.297 |
| 5 | $P_2O_5$ | 0.736 | 0.012 | 0.233 |
| 6 | $SO_3$ | 2.669 | 54.354 | 5.745 |
| 7 | CaO | 10.072 | 18.810 | 18.129 |
| 8 | MgO | 33.318 | 0.000 | 38.006 |
| 9 | $K_2O$ | 7.057 | 0.158 | 1.723 |
| 10 | $Al_2O$ | 7.759 | 5.071 | 6.138 |
| 11 | TiO2 | 0.349 | 0.233 | 0.268 |
| 12 | ZnO | 0.168 | 0.394 | 0.222 |
| 13 | Cl | 13.902 | 6.877 | 7.396 |

### 3.2 Sample Characterisation

The experimental results obtained from sample characterisation of cow hair fibre based ceiling boards (CHF) and snot apple fibre based ceiling boards (SAF) are presented in Table 4 while the results of Signal to noise (SN) ratios for CHF and SAF are presented in Table 5. The SN ratios for tensile strength, hardness and impact energy were conducted using larger-the-better (Equation 3) while SN ratios for water absorption and thickness swelling was calculated using smaller-the-better quality characteristics (Equation 4). Table 4 shows that Cow Hair Fibre (CHF) exhibits consistent tensile strength (7.3–11.92 MPa), hardness (57.27–94.3 HVN), impact energy (0.15–0.32 J), higher water absorption, and lower thickness swelling, while Snot Apple Fibre (SAF) displays greater variability with tensile strength ranging from 5.97 to 31.81 MPa,

hardness from 62.73 to 98.23 HVN, impact energy from 0.37 to 1.22 J, generally lower water absorption, but consistently higher thickness swelling-indicating SAF's potential for superior mechanical performance under optimal conditions [16].

$$\text{Small-the better: } S/N = -10\log\frac{1}{n}\left(\sum_{i-1}^{n} y_i^2\right) \quad (3)$$

$$\text{Larger-the better: } S/N = -10\log\frac{1}{n}\left(\sum_{i-1}^{n} 1/y_i^2\right) \quad (4)$$

Where; y = given factor level combination responses; n = number of factor level combination responses

Table 4: Experimental results of CHF and SAF

| Run | CHF | | | | | SAF | | | | |
|---|---|---|---|---|---|---|---|---|---|---|
| | Tensile (MPa) | Hardness (HVN) | Impact (J) | Water Absorption (%) | Thickness Swelling (%) | Tensile (MPa) | Hardness (HVN) | Impact (J) | Water Absorption (%) | Thickness Swelling (%) |
| 1 | 11.37 | 57.27 | 0.15 | 7.183 | 4.695 | 15.34 | 62.73 | 0.37 | 3.864 | 3.864 |
| 2 | 9.53 | 65.17 | 0.16 | 5.88 | 5.443 | 31.81 | 71.8 | 0.38 | 2.878 | 2.878 |
| 3 | 7.46 | 71.57 | 0.25 | 13.075 | 4.178 | 10.21 | 85.07 | 0.98 | 11.025 | 11.025 |
| 4 | 7.59 | 82.17 | 0.20 | 8.871 | 2.29 | 12.42 | 87.07 | 0.52 | 9.602 | 13.066 |
| 5 | 11.915 | 66.73 | 0.32 | 9.547 | 5.844 | 8.67 | 71.10 | 0.70 | 8.749 | 8.749 |
| 6 | 11.38 | 88.77 | 0.23 | 5.012 | 2.178 | 5.97 | 94.33 | 0.55 | 9.960 | 9.802 |
| 7 | 8.122 | 75.13 | 0.15 | 11.651 | 6.399 | 9.66 | 83.63 | 0.83 | 9.390 | 9.390 |
| 8 | 7.30 | 80.47 | 0.31 | 13.816 | 3.384 | 8.91 | 70.30 | 1.22 | 6.424 | 6.424 |
| 9 | 8.94 | 94.3 | 0.18 | 8.202 | 2.682 | 9.60 | 98.23 | 0.57 | 7.038 | 3.566 |

Table 5: Signal to Noise ratios of CHF and SAF

| Run | CHF | | | | | SAF | | | | |
|---|---|---|---|---|---|---|---|---|---|---|
| | Tensile (dB) | Hardness (dB) | Impact (dB) | Water Absorption (dB) | Thickness Swelling (dB) | Tensile (dB) | Hardness (dB) | Impact (dB) | Water Absorption (dB) | Thickness Swelling (dB) |
| 1 | 21.115 | 35.159 | -16.478 | -17.126 | -13.433 | 23.717 | 35.950 | -8.636 | -11.742 | -11.741 |
| 2 | 19.582 | 36.281 | -15.918 | -15.388 | -14.717 | 30.051 | 37.122 | -8.404 | -9.181 | -9.182 |
| 3 | 17.455 | 37.095 | -12.041 | -22.329 | -12.419 | 20.181 | 38.596 | -0.175 | -20.847 | -20.848 |
| 4 | 17.605 | 38.294 | -13.979 | -18.959 | -7.197 | 21.882 | 38.797 | -5.680 | -19.647 | -22.323 |
| 5 | 21.522 | 36.486 | -9.897 | -19.597 | -15.334 | 18.760 | 37.037 | -3.098 | -18.839 | -18.839 |
| 6 | 21.123 | 38.965 | -12.765 | -14.000 | -6.761 | 15.519 | 39.493 | -5.193 | -19.965 | -19.826 |
| 7 | 18.193 | 37.516 | -16.478 | -21.327 | -16.122 | 19.700 | 38.447 | -1.618 | -19.453 | -19.453 |
| 8 | 17.266 | 38.113 | -10.173 | -22.808 | -10.589 | 18.998 | 36.939 | 1.727 | -16.156 | -16.156 |
| 9 | 19.027 | 39.490 | -14.895 | -18.278 | -8.569 | 19.645 | 39.845 | -4.883 | -16.950 | -11.044 |

### 3.3 Analysis of Experimental results

#### 3.3.1 Main effects plots

The main effect plots in Figure 3a and 3b indicate that filler content (g) has the greatest influence on the mean signal-to-noise (SN) ratios for tensile strength of both CHF and SAF, with peak SN ratios at 40g for CHF and 30g for SAF, demonstrating a strong sensitivity to filler levels. In comparison, coconut shell (g) and binder (g) show only minor effects with slight variations across their levels, suggesting a less pronounced impact on tensile strength. Overall, optimal tensile strength is achieved with 40g filler, 90g coconut shell, and 110g epoxy resin binder for CHF, and 30g filler, 90g coconut shell, and 110g binder for SAF. Similarly, Figure 4a and 4b reveal that filler (g) most significantly affects the hardness of CHF, while coconut shell (g) is the key factor for SAF hardness, with highest SN ratios at 50g filler for CHF and 100g coconut shell for SAF. Although filler and binder show minor effects on SAF hardness (Figure 5b), slight variations suggest some influence on CHF hardness (Figure 5a). The optimal hardness conditions are 50g filler, 100g coconut shell, and 110g binder for CHF, and 40g filler, 100g coconut shell, and 110g binder for SAF. Also. for impact energy, Figure 5a and 6b show coconut shell (90g) has the most significant impact on CHF, while binder (120g) is most influential for SAF, with minor effects observed for binder on CHF and coconut shell on SAF. Optimal impact energy was achieved with 40g filler, 90g coconut shell, and 120g binder for CHF, and 50g filler, 90g coconut shell, and 120g binder for SAF.

The main effect plots for water absorption presented in Figure 6a and 6b shows epoxy resin binder as the dominant factor for both CHF and SAF, with highest SN ratios at 110g and 100g respectively, indicating strong sensitivity to binder content. Filler and coconut shell show only slight effects. Optimal water absorption occurs at 40g filler, 100g coconut shell, and 110g binder for CHF, and 30g filler, 90g coconut shell, and 110g binder for SAF. Finally, Figure 7a and 7b demonstrate that epoxy resin binder (110g) most significantly affects thickness swelling of CHF, whereas filler (30g) is the key factor for SAF. Minor effects are observed for filler and coconut shell in CHF and SAF respectively. Optimal thickness swelling is achieved with 40g filler, 100g coconut shell, and 110g binder for CHF, and 30g filler, 90g coconut

shell, and 100g binder for SAF. Abutu et al. [10] emphasize that changes in these optimal parameters could impact the performance of the developed ceiling boards.

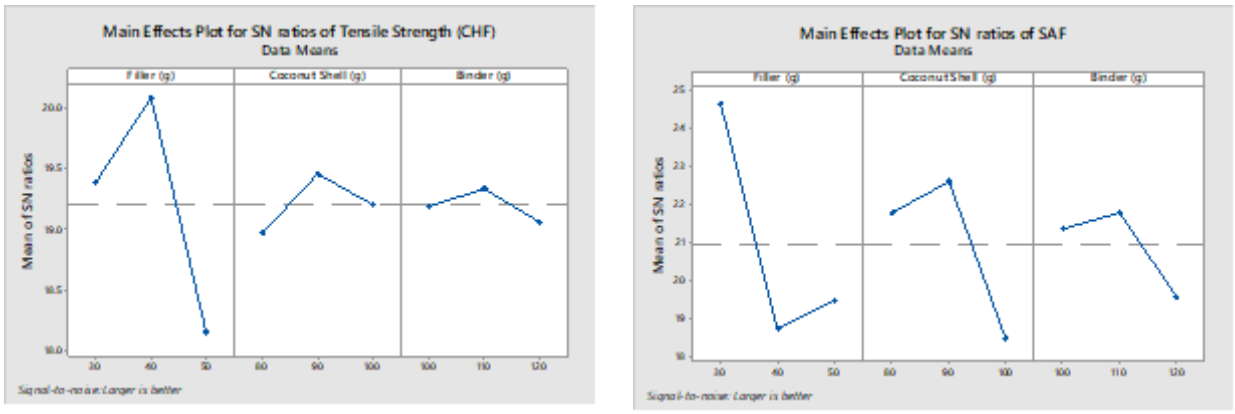


(a) (b)

Figure 3: Main effects plot for Tensile strength (a) CHF (b) SAF

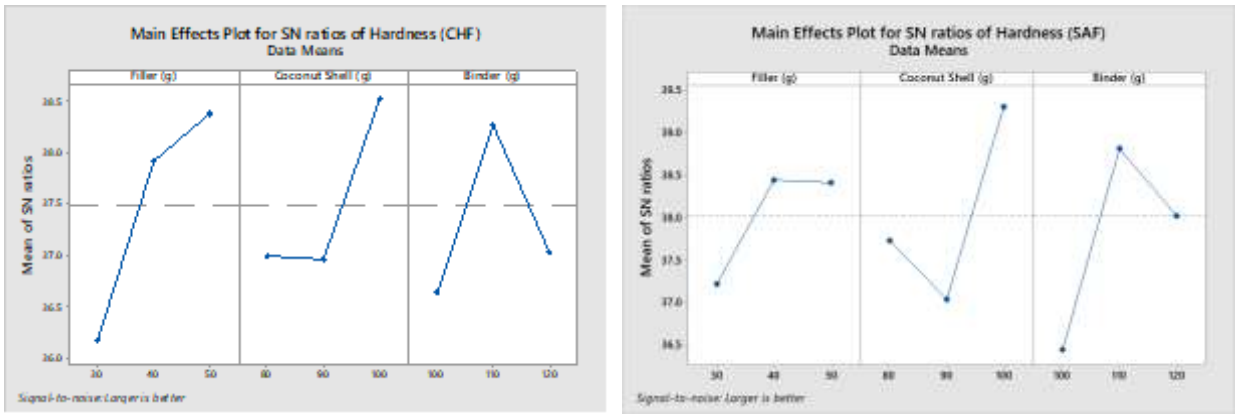


(a) (b)

Figure 4: Main effects plot for Hardness (a) CHF (b) SAF

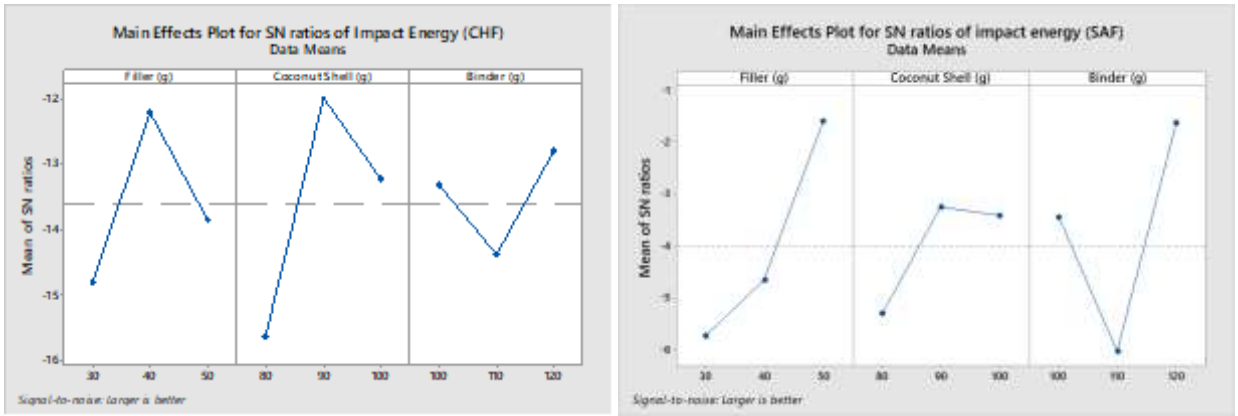


(a) (b)

Figure 5: Main effects plot for impact energy (a) CHF (b) SAF

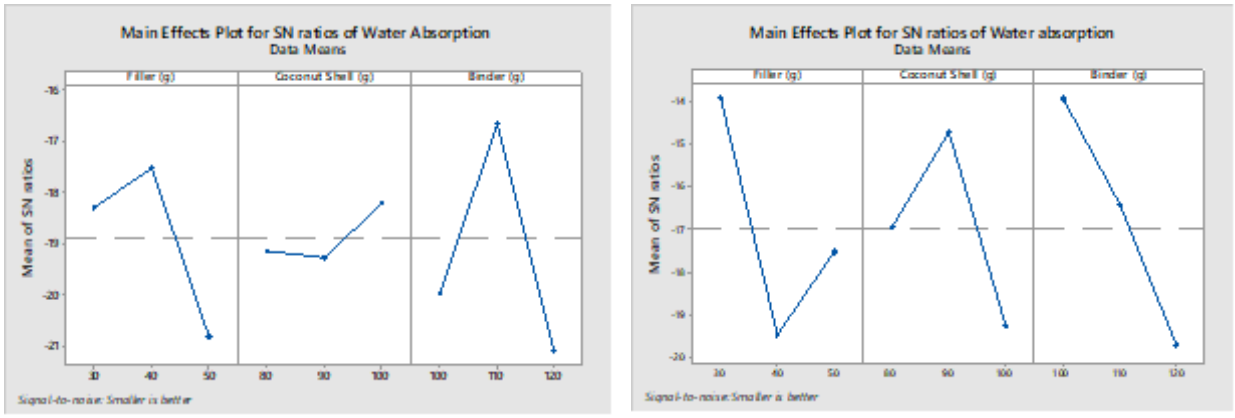


(a) (b)

Figure 6: Main effects plot for water absorption (a) CHF (b) SAF

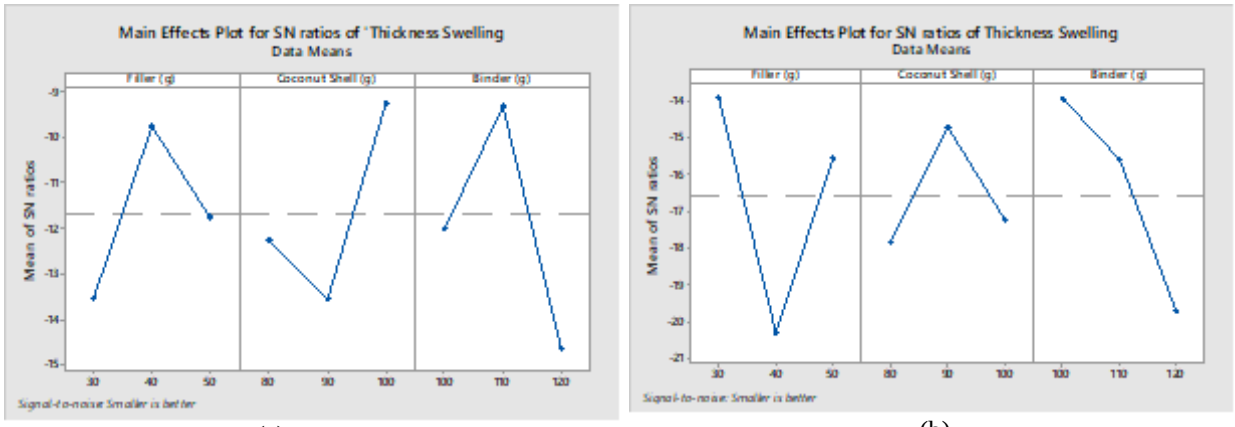


(a) (b)

Figure 7: Main effects plot for thickness swelling (a) CHF (b) SAF

### 3.3.2 Analysis of variance

Analysis of variance (ANOVA) was conducted in order to identify the significant effects (relative importance) of the experimental parameters (input factors) which affect the quality characteristics of the developed ceiling boards. The significant effects of each parameter were given the order of their percentage contribution which was calculated during this analysis. As recommended by Irechukwu et al. [17], the analysis was conducted for $\alpha$ = 0.05 significance level, at 95 % confidence level. Equation 5 was utilised for calculation of total sum of square while the ANOVA for each response is shown in Table 6-10.

$$\text{Sum of Square } (SS_{Total}) = \sum_{i=1}^{n} y_i^2 - \frac{i}{n}(y_i)^2 \qquad (i = 1, 2, 3\ldots\ldots, 9) \qquad (5)$$

The results in Table 6 show that filler, coconut shells, and binder all significantly influence the tensile strength of both CHF and SAF, with filler having the greatest impact (48.4% for CHF and 50.07% for SAF) supported by high F-values (8.36 and 19.51 respectively), followed by coconut shells (23.7% for CHF and 28.11% for SAF), while epoxy resin binder has the least effect (22.2% for CHF and 19.25% for SAF); low error rates (5.79% for CHF and 2.57% for SAF) indicate a strong model fit and minimal experimental noise. Also, Table 7 indicates that all factors significantly affect hardness in both materials, with filler most influential for CHF hardness (44.74%, F-value 12.45) and coconut shells for SAF hardness (50.18%, F-value 45.61), followed by coconut shells for CHF (27.22%) and binder for SAF (40.28%), while epoxy resin binder and filler have the least influence on CHF (22.2%) and SAF (8.43%) hardness respectively; low errors (3.59% for CHF and 1.10% for SAF) confirm reliable models. However, according to Table 8, all factors significantly affect impact energy, with coconut shells having the largest effect on CHF (49.62%, F-value 18.20) and binder on SAF (43.80%, F-value 17.41), followed by filler (26.36% for CHF and 35.42% for SAF), while binder and coconut shells have the least influence on CHF (21.29%) and SAF (18.27%) respectively; low errors (2.73% for CHF and 2.52% for SAF) suggest strong model accuracy.

In addition, Table 9 revealed that epoxy resin binder most strongly affects water absorption in both CHF (56.08%, F-value 13.24) and SAF (40.38%, F-value 8.91), followed by filler (31.21% for CHF and 29.08% for SAF), with coconut shells having the least effect (8.48% for CHF and 26.01% for SAF); low errors (4.23% for CHF and 4.53% for SAF) indicate minimal noise in the experiments. Finally, Table 10 shows that epoxy resin binder predominantly influences thickness swelling in CHF (48.48%, F-value 9.61), while filler has the greatest effect on SAF (44.09%, F-value 10.73), followed by coconut shells for CHF (31.07%) and binder for SAF (32.27%), with filler and coconut shells having the least influence on CHF (15.40%) and SAF (19.53%) respectively; low error values (5.05% for CHF and 4.11% for SAF) confirm strong model fits and minimal noise during testing.

Table 6: ANOVA for tensile strength

| | CHF | | | | | SAF | | | | |
|---|---|---|---|---|---|---|---|---|---|---|
| Factor | DOF | SS | MS | F | P(%) | DOF | SS | MS | F | P(%) |
| Filler (g) | 2 | 13.21 | 6.606 | 8.36 | 48.4 | 2 | 236.8 | 118.4 | 19.51 | 50.07 |
| Coconut Shell (g) | 2 | 6.465 | 3.232 | 4.09 | 23.7 | 2 | 132.9 | 66.46 | 10.95 | 28.11 |
| Binder (g) | 2 | 6.070 | 3.035 | 3.84 | 22.2 | 2 | 91.05 | 45.53 | 7.500 | 19.25 |
| Error | 2 | 1.581 | 0.791 | | 5.79 | 2 | 12.14 | 6.070 | | 2.57 |
| Total | 8 | 27.33 | 3.416 | | 100 | 8 | 472.9 | 59.11 | | 100.00 |

Table 7: ANOVA for hardness

| | CHF | | | | | SAF | | | | |
|---|---|---|---|---|---|---|---|---|---|---|
| Factor | DOF | SS | MS | F | P(%) | DOF | SS | MS | F | P(%) |
| Filler (g) | 2 | 505.5 | 252.75 | 12.45 | 44.74 | 2 | 98.1 | 49.05 | 7.66 | 8.43 |
| Coconut Shell (g) | 2 | 307.5 | 153.75 | 7.574 | 27.22 | 2 | 583.8 | 291.9 | 45.61 | 50.18 |
| Binder (g) | 2 | 276.2 | 138.1 | 6.803 | 24.45 | 2 | 468.6 | 234.3 | 36.61 | 40.28 |
| Error | 2 | 40.6 | 20.3 | | 3.59 | 2 | 12.8 | 6.4 | | 1.10 |
| Total | 8 | 1129.8 | 141.23 | | 100 | 8 | 1163.3 | 145.4 | | 100 |

Table 8: ANOVA for impact energy

| | CHF | | | | | SAF | | | | |
|---|---|---|---|---|---|---|---|---|---|---|
| Factor | DOF | SS | MS | F | P(%) | DOF | SS | MS | F | P(%) |
| Filler (g) | 2 | 0.0091 | 0.0045 | 9.67 | 26.36 | 2 | 0.229 | 0.114 | 14.08 | 35.42 |
| Coconut Shell (g) | 2 | 0.0171 | 0.0085 | 18.20 | 49.62 | 2 | 0.118 | 0.059 | 7.26 | 18.27 |
| Binder (g) | 2 | 0.0073 | 0.0037 | 7.81 | 21.29 | 2 | 0.283 | 0.141 | 17.41 | 43.80 |
| Error | 2 | 0.0009 | 0.0005 | | 2.73 | 2 | 0.016 | 0.008 | | 2.52 |
| Total | 8 | 0.0344 | 0.0043 | | 100 | 8 | 0.645 | 0.081 | | 100 |

Table 9: ANOVA for water absorption

| | CHF | | | | | SAF | | | | |
|---|---|---|---|---|---|---|---|---|---|---|
| Factor | DOF | SS | MS | F | P(%) | DOF | SS | MS | F | P(%) |
| Filler (g) | 2 | 23.77 | 11.89 | 7.371 | 31.21 | 2 | 18.54 | 9.27 | 6.415 | 29.08 |
| Coconut Shell (g) | 2 | 6.455 | 3.228 | 2.002 | 8.48 | 2 | 16.58 | 8.29 | 5.737 | 26.01 |
| Binder (g) | 2 | 42.71 | 21.36 | 13.24 | 56.08 | 2 | 25.74 | 12.87 | 8.907 | 40.38 |
| Error | 2 | 3.225 | 1.613 | | 4.23 | 2 | 2.890 | 1.445 | | 4.53 |
| Total | 8 | 76.16 | 9.52 | | 100 | 8 | 63.75 | 7.969 | | 100. |

Table 10: ANOVA for thickness swelling

| | CHF | | | | | SAF | | | | |
|---|---|---|---|---|---|---|---|---|---|---|
| Factor | DOF | SS | MS | F | P(%) | DOF | SS | MS | F | P(%) |
| Filler (g) | 2 | 3.077 | 1.54 | 3.05 | 15.40 | 2 | 46.24 | 23.120 | 10.73 | 44.09 |
| Coconut Shell (g) | 2 | 6.208 | 3.10 | 6.16 | 31.07 | 2 | 20.48 | 10.240 | 4.752 | 19.53 |
| Binder (g) | 2 | 9.687 | 4.84 | 9.61 | 48.48 | 2 | 33.85 | 16.925 | 7.854 | 32.27 |
| Error | 2 | 1.01 | 0.50 | | 5.05 | 2 | 4.31 | 2.155 | | 4.11 |
| Total | 8 | 19.98 | 2.50 | | 100 | 8 | 104.88 | 13.110 | | 100. |

### 3.3.3 Contour plots

Contour plots, were generated using Minitab 19, which graphically represent the relationships between two input variables and a single output variable by displaying 3-dimensional relationships on a 2-dimensional plane, where experimental factors are plotted on the axes and response values are represented by contours. The contour plots in Figures. 8 to 12 indicate how filler and binder contents affect various properties of CHF and SAF ceiling boards, with coconut shell content fixed at 90g, highlighting the complex interactions between filler and binder. Specifically, Figure 8a shows that tensile strength above 14 MPa for CHF is achieved with 30–35g filler (cow hair fibre) and 100g binder, while Figure 8b indicates that SAF reaches tensile strength over 30 MPa with 30g filler (snot apple fibre) and 109–111g binder. Figure 9a reveals hardness greater than 80 HVN for CHF at 50g filler and binder ranging from 50 to 112g, whereas Figure 9b shows SAF hardness above 80 HVN with 50g filler and 107–112g binder. In Figure 10a, impact energy exceeding 0.32 J for CHF is attained with 40–47g filler and 50g binder, while Figure 10b indicates SAF achieves 1.0 to 1.2 J impact energy with 45–50g filler and 100g binder. Figure 11a shows water absorption below 4% for CHF with 30–32g filler and 100–105g binder, and Figure 11b reveals SAF attains less than 2% absorption with 30g filler and 100–103g binder. Finally, Figure 12a illustrates thickness swelling under 4% for CHF at 40–50g filler and 100–105g binder, while Figure 12b indicates SAF achieves swelling below 2% with 30g filler and 100–103g binder. These plots highlight the intricate balance between filler and binder contents required to optimize the mechanical and physical properties of both materials.

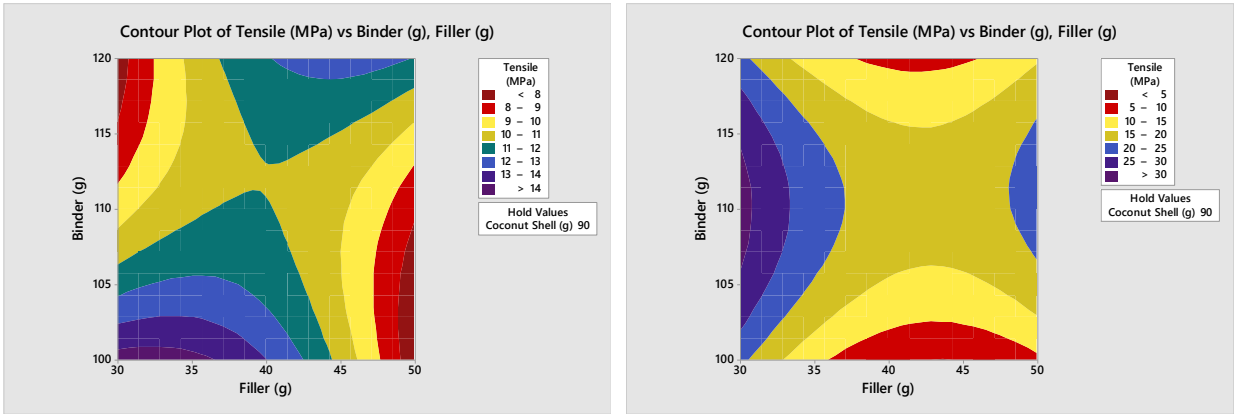


(a) (b)

Figure 8: Contour plot for Tensile strength (a) CHF (b) SAF

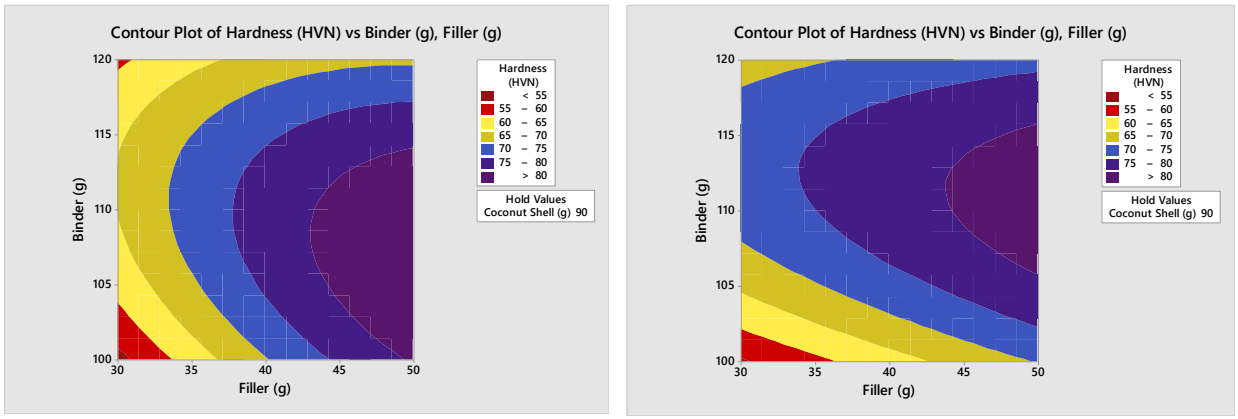


(a) (b)

Figure 9: Contour plot for Hardness (a) CHF (b) SAF

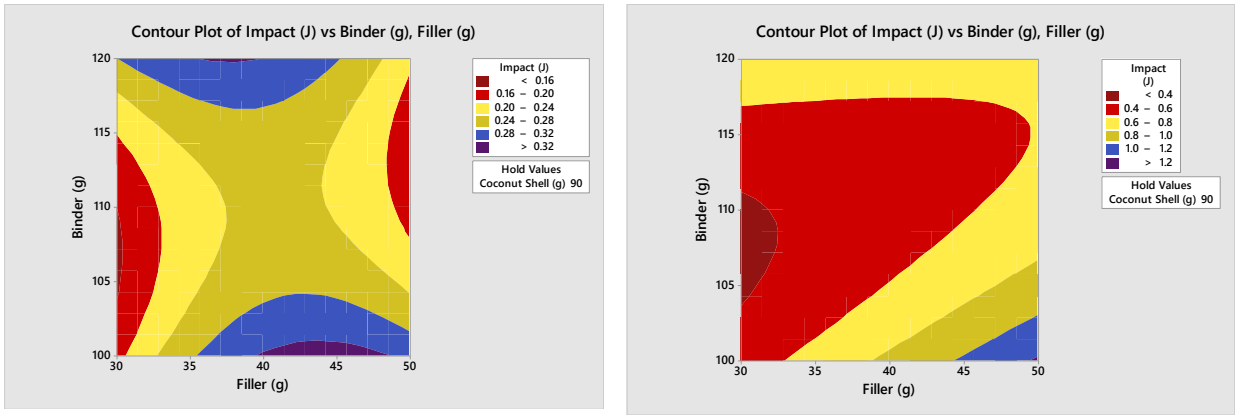


(a) (b)

Figure 10: Contour plot for impact energy (a) CHF (b) SAF

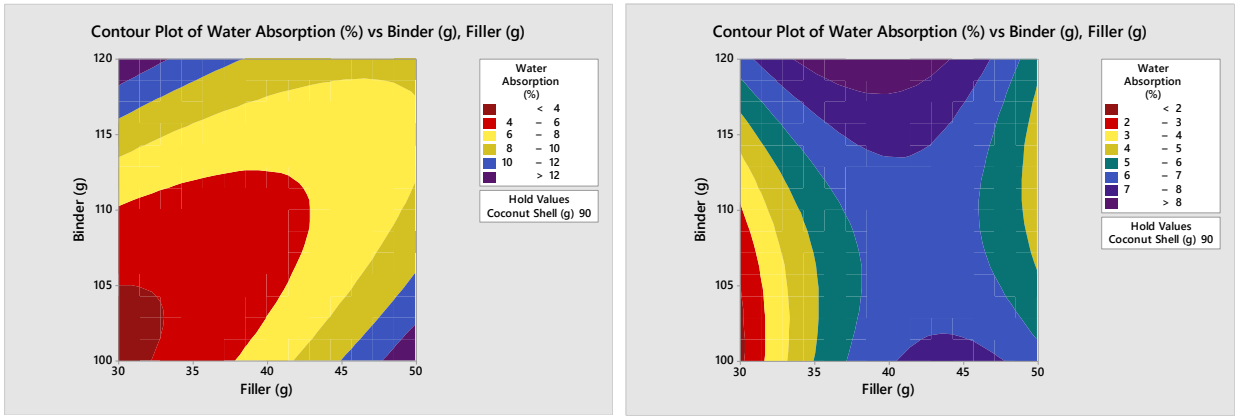


(a) (b)

Figure 11: Contour plot for plot for Water absorption (a) CHF (b) SAF

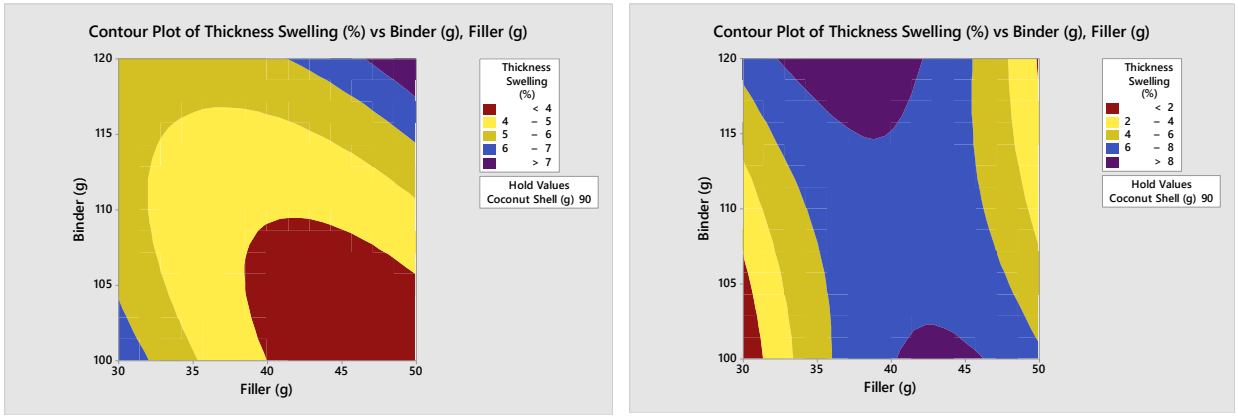


(a) (b)

Figure 12: Contour plot for thickness swelling (a) CHF (b) SAF

### 3.3.4 Empirical regression models

Empirical model equations for predicting tensile strength (T), hardness (H), impact energy (IE), water absorption (WA), and thickness swelling (TS) were developed using Minitab 19 statistical software. These models describe how the response variables change in relation to the independent variables-filler ($\gamma$), coconut shell ($\beta$), and binder ($\alpha$). The equations for CHF are presented in Equations 6 to 10, while those for SAF are given in Equations 11 to 15. Although some adjusted R-

squared (Rsq(adj)) values are below 80%, this is likely due to experimental uncertainties arising from uncontrollable factors, as noted by Irechukwu et al. [17].

**a. Cow hair fibre-based ceiling board (CHF)**

i. $T\ (MPa) = 39 + 1.42\ \gamma + 0.50\ \beta - 1.39\ \propto - 0.0186\ \gamma * \gamma - 0.0026\ \beta * \beta + 0.0061\ \propto * \propto$ (6)
Rsq = 92.00%, Rsq (adj) = 81.09%

ii. $Hs\ (HVN) = -462 + 3.42\ \gamma - 10.87\ \beta + 16.79\ \propto - 0.0311\ \gamma * \gamma + 0.0635\ \beta * \beta - 0.0769\ \propto * \propto$ (7)
Rsq = 95.93%, Rsq (adj) = 83.73%

iii. $IE\ (J) = 4.30 + 0.0673\ \gamma + 0.1010\ \beta - 0.1830\ \propto - 0.000825\ \gamma * \gamma - 0.000538\ \beta * \beta + 0.000825\ \propto * \propto$ (8)
Rsq = 90.21%, Rsq (adj) = 80.85%

iv. $WA\ (\%) = 439 - 0.77\ \gamma + 0.45\ \beta - 8.07\ \propto + 0.0113\ \gamma * \gamma - 0.0023\ \beta * \beta + 0.0370\ \propto * \propto$ (9)
Rsq = 89.96%, Rsq (adj) = 79.83%

v. $TS\ (\%) = -16 - 1.033\ \gamma + 2.20\ \beta - 1.11\ \propto + 0.01253\ \gamma * \gamma - 0.01267\ \beta * \beta + 0.00561\ \propto * \propto$ (10)
Rsq = 85.71% and Rsq (adj) = 72.84%

**b. Snot apple fibre based ceiling board (SAF)**

i. $T\ (MPa) = -1733 - 8.027\ \gamma + 14.04\ \beta + 23.57\ \propto + 0.09425\ \gamma * \gamma - 0.08025\ \beta * \beta - 0.10627\ \propto * \propto$ (11)
Rsq = 99.52%, Rsq (adj) = 98.08%

ii. $H\ (HVN) = -300 + 1.17\ \gamma - 20.62\ \beta + 22.27\ \propto - 0.0078\ \gamma * \gamma + 0.1173\ \beta * \beta - 0.0992\ \propto * \propto$ (12)
Rsq = 98.38%%, Rsq (adj) = 93.51%

iii. $IE\ (J) = 36.3 + 0.002\ \gamma + 0.139\ \beta - 0.781\ \propto + 0.00016\ \gamma * \gamma - 0.00071\ \beta * \beta + 0.00355\ \propto * \propto$ (13)
Rsq = 89.68%, Rsq (adj) = 80.21%

iv. $WA\ (\%) = 373 + 2.37\ \gamma - 4.50\ \beta - 4.08\ \propto - 0.0285\ \gamma * \gamma + 0.0256\ \beta * \beta + 0.0192\ \propto * \propto$ (14)
Rsq = 85.54%, Rsq (adj) = 72.15%

v. $TS\ (\%) = 358 + 3.65\ \gamma - 4.57\ \beta - 4.08\ \propto - 0.0453\ \gamma * \gamma + 0.0252\ \beta * \beta + 0.0192\ \propto * \propto$ (15)
Rsq = 87.18%%, Rsq (adj) = 71.88%

### 3.4 Microstructural Examination

The microstructures of the optimized fractured samples from the tensile test are shown in Figure 13a (CHF) and Figure 13b (SAF). The SEM image of the CHF sample (Figure 13a) at 500x magnification reveals an irregular, granular morphology with a heterogeneous microstructure and a wide distribution of particle sizes, indicating the presence of multiple phases. The observed agglomeration of finer particles is likely due to surface and capillary forces, such as liquid bridges between particles, as well as preferential clustering during mixing [19-20]. In contrast, the SEM image of the SAF sample (Figure 13b), also at 500x magnification, shows fibrous elements embedded within an epoxy resin matrix. These fibres exhibit distinct longitudinal striations reflecting their natural texture and alignment, while the surrounding matrix appears rough and granular. The clear presence of well-distributed fibres with strong interfacial bonding within the matrix confirms that the developedSAF is a true composite material, where natural fibres are effectively integrated into the epoxy binder, enhancing the composite's mechanical and physical [10].

### 3.5 Thermal analysis

The Thermogravimetric Analysis (TGA) results are illustrated in Figures 14. The temperature range applied in this study remains below the degradation temperatures of all components in the optimized ceiling board samples. During the initial stability phase (up to 350°C), both the SAF and CHF samples exhibit minimal weight loss, indicating good thermal stability and the absence of volatile substances or moisture. Notably, the onset of decomposition occurs earlier for the CHF sample, which begins to lose weight rapidly just after 350°C, whereas the SAF sample starts to degrade later, around 450°C. Between 350°C and 600°C, CHF undergoes a sharp weight loss, resulting in approximately 15% residue remaining by 700°C. In contrast, SAF experiences a more gradual weight loss beginning at 450°C and stabilizes at about 60% residue near 750°C. The substantial residue of SAF (60%) at 900°C suggests a higher proportion of thermally stable or inorganic components, likely due to the inherent stability of the snot apple fibre. At 900°C, SAF retains around 60% of its original mass, while CHF retains only about 15%. These findings indicate that the higher decomposition onset temperature of SAF

(450°C) implies that the combination of snot apple fibre with coconut shell powder and epoxy resin offers superior thermal stability compared to the CHF ceiling board sample, which begins degrading at a lower temperature (350°C). Table 11 presents the detailed data for the optimized SAF and CHF ceiling board samples.

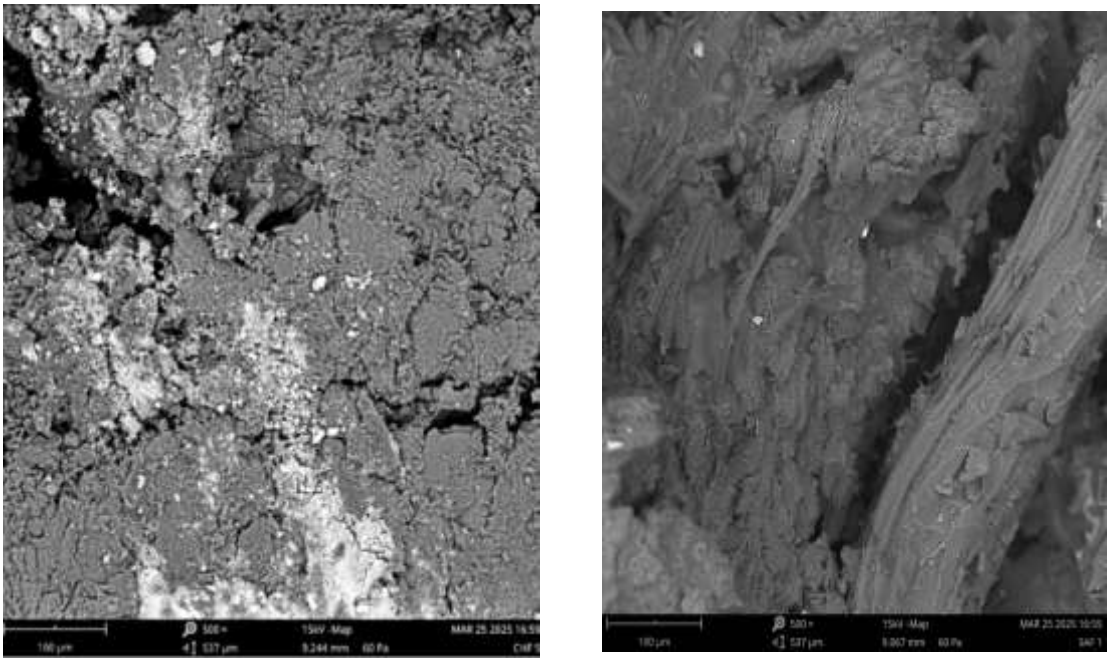

(a) (b)

Figure 13: SEM image of optimized (a) CHF (b) SAF

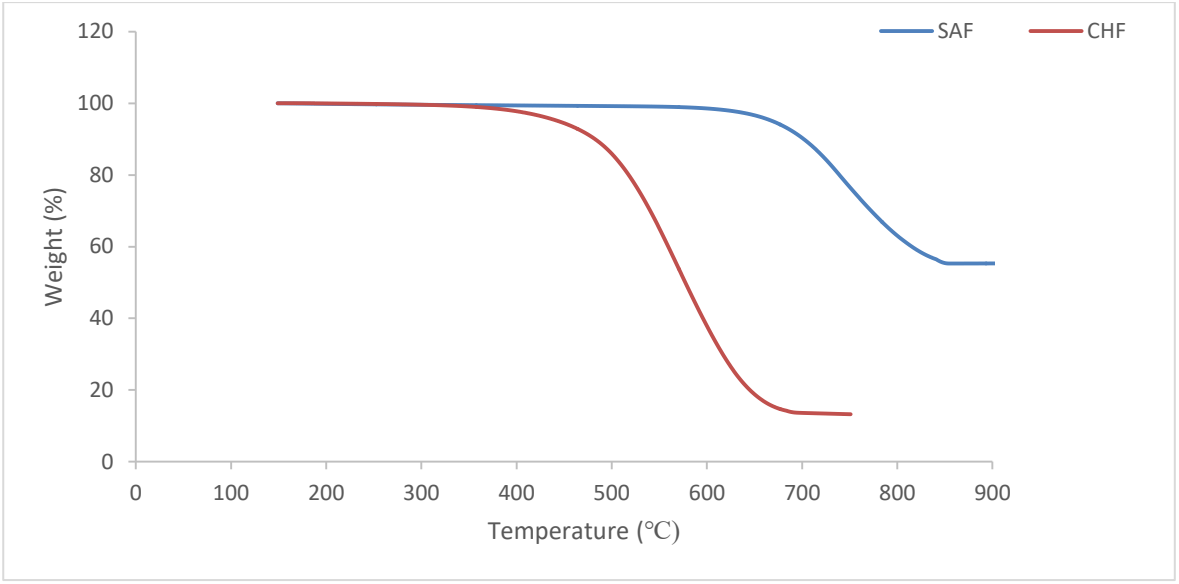


Figure 14: TGA of optimized samples

Table 11: TGA data for optimised SAF and CHF ceiling board samples

| Feature | SAF | CHF |
|---|---|---|
| Onset Temperature | 450°C | 350°C |
| Major Weight Loss | 450°C–700°C | 350°C–600°C |
| Residual Weight | 60% at 900°C | 10% at 900°C |
| Peak degradation temperature | 620 °C | 550 °C |

The Derivative Thermogravimetric (DTG) analysis results for the Cow Hair Fibre (CHF) and Snot Apple Fibre (SAF) composites, as illustrated in Figure 15, demonstrate the thermal degradation behaviour of these materials. This analysis not only confirms the thermal degradation stages of CHF and SAF composites but also allows for a comparative assessment of their thermal performance, which is crucial for determining their suitability in applications as ceiling board where thermal resistance is a key requirement. Initially, both samples retain approximately 100% of their original weight, indicating no mass loss at lower temperatures. As the temperature increases, the samples begin to lose mass progressively due to thermal decomposition. Notably, the onset temperature (the point at which significant degradation begins) differs markedly between the two composites. The CHF composite starts to degrade at around 180°C, whereas the SAF composite exhibits a much higher onset temperature of approximately 540°C. This substantial difference suggests that SAF has a considerably higher resistance to thermal degradation. Also, the peak degradation temperature, which corresponds to the temperature at which the rate of mass loss is at its maximum, also varies between the two ceiling board samples. The CHF composite reaches its peak degradation rate at about 420°C, while the SAF composite peaks at a significantly higher temperature of roughly 660°C. These findings clearly indicate that the SAF composite possesses superior thermal stability compared to the CHF composite. This enhanced thermal stability of SAF can be attributed to its intrinsic fibre composition. According to Mann et al. [18], snot apple fibre contains a higher concentration of thermally stable constituents such as cellulose, lignin, and other biopolymers. In contrast, cow hair fibre, which is protein-rich, tends to degrade at lower temperatures. The presence of these more resilient biopolymers in SAF contributes to its ability to withstand elevated temperatures without significant degradation.

From an application perspective, the higher thermal stability of SAF composites makes them ideal for use in high-temperature environments. In contrast, although CHF composites exhibit lower thermal stability, this is compensated by their superior biodegradability and cost-effectiveness, making them well-suited for less demanding thermal applications. Therefore, these thermal properties suggest that SAF composites are preferable in settings where exposure to elevated temperatures is expected or unavoidable, while CHF composites are more appropriate for environments with lower thermal requirements. Moreover, the biodegradability and affordability of CHF composites provide additional benefits, making them a practical choice when thermal resistance is not a primary concern. Detailed DTG data for the optimized SAF and CHF ceiling board samples are presented in Table 12.

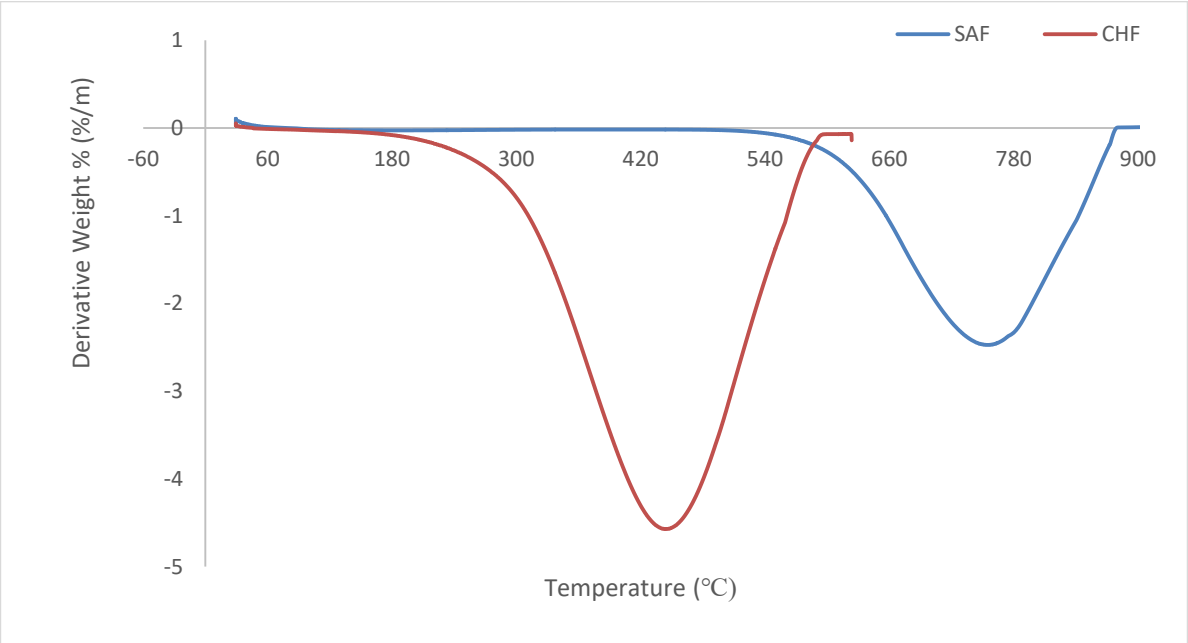


Figure 15: DTG of optimized ceiling board samples

Table 12: DTG data for optimised SAF and CHF ceiling board samples

| Ceiling Board sample | Onset Temp (°C) | Degradation Range (°C) | Peak Temperature (°C) |
|---|---|---|---|
| CHF | 180 | 180–540 | 420 |
| SAF | 540 | 540–900 | 660 |

## 4. CONCLUSION

In this study, coconut shells, cow hair, and snot apple fibres were locally sourced as organic wastes and analyzed for their elemental composition. Ceiling boards were then fabricated using the Taguchi design method, and the resulting samples were characterized. Based on the results obtained, the following conclusions can be made:

i. The XRF analysis revealed that coconut shell fibre is dominated by magnesium oxide (MgO), silicon dioxide ($SiO_2$), calcium oxide (CaO), and chlorine (Cl), suggesting a magnesium silicate-like structure suitable for composite applications. Cow hair fibre is sulfate-rich ($SO_3$) with significant CaO, indicating a different chemical environment, while snot apple fibre is magnesium-rich with substantial $SiO_2$ and CaO, resembling talc or serpentinite.
ii. Variations in experimental parameters significantly influence the performance characteristics, including hardness, tensile strength, impact energy, water absorption, and thickness swelling, of the composite samples, as demonstrated by the differing results across all test runs.
iii. Snot apple fibre-based boards (SAF) demonstrated superior tensile strength (12.51 MPa) and hardness (79.5 HVN) compared to cow hair fibre-based boards (CHF: 9.29 MPa, 73.3 HVN), along with higher impact energy (0.68 J vs. 0.22 J), but exhibited greater variability in mechanical performance and dimensional instability through thickness swelling when exposed to moisture, while CHF showed more consistent results despite higher water absorption.
iv. The Analysis of Variance results revealed that filler content predominantly influences tensile strength and hardness in cow hair fibre-based boards (CHF), whereas coconut shell and binder content are key for snot apple fibre-based boards (SAF), with epoxy resin binder critically affecting water absorption and thickness swelling in both materials, necessitating distinct optimal parameter formulations for CHF and SAF depending on target performance metrics.
v. The developed composite material demonstrates suitability for adoption as ceiling boards in structural applications, offering a combination of mechanical strength (including tensile strength and hardness), impact resistance, and moisture management properties critical for load-bearing and environmental resilience in building systems.
vi. The SAF ceiling board demonstrates significantly superior thermal stability compared to the CHF composite, making it more suitable for high-temperature applications, while CHF offers advantages in biodegradability and cost for less thermally demanding uses.

## REFERENCES

[1] Guredam, L. A. L., & Ossia, C. V. (2024). Advancements in Using Organic Waste Materials for Green Composites in Ceiling Board Applications: A Mini Review, World scientific news, 196,114-133.
[2] Adebawo, F. G., Okon-Akan, O. A., & Olaoye, K. O. (2019). Assessment Of Mechanical Properties Of Ceiling Board Produced From Gypsum Reinforced With Natural Fibre, Journal of Forestry Research and Management, 16(2).138-147.
[3] Al-Azad, N., Asril, M. F. M., & Shah, M. K. M. (2021). A review on development of natural fibre composites for construction applications. *Journal of Materials Science and Chemical Engineering*, *9*(7), 1-9.
[4] Guredam, L. A. L., & Ossia, C. V. (2024). Advancements in Using Organic Waste Materials for Green Composites in Ceiling Board Applications: A Mini Review. World Scientific News, 196, 114–133. EISSN 2392-2192.
[5] Thyavihalli G. Y. G., Mavinkere Rangappa, S., Parameswaranpillai, J., & Siengchin, S. (2019). Natural fibres as sustainable and renewable resource for development of eco-friendly composites: a comprehensive review. *Frontiers in materials*, *6*, 226.
[6] Celadyn, M. (2018). Environmental activation of inner space components in sustainable interior design. *Sustainability*, *10*(6), 1945.
[7] Sanjay, M. R., Arpitha, G. R., Naik, L. L., Gopalakrishna, K., & Yogesha, B. J. N. R. (2016). Applications of natural fibres and its composites: an overview. *Natural resources*, *7*(3), 108-114.
[8] Carcassi, O. B., Minotti, P., Habert, G., Paoletti, I., Claude, S., & Pittau, F. (2022). Carbon footprint assessment of a novel bio-based composite for building insulation. *Sustainability*, *14*(3), 1384.
[9] Oladele, I. O., Ibrahim, I. O., Adediran, A. A., Akinwekomi, A. D., Adetula, Y. V., & Olayanju, T. M. A. (2020). Modified palm kernel shell fibre/particulate cassava peel hybrid reinforced epoxy composites. *Results in materials*, *5*, 100053.
[10] Abutu, J., Tsoji, T. R., Stephen, A., Araye, A. D., Lawal, S. A., & Rimamtaatang, A. K. (2024). Performance assessment of particle board developed from organic wastes using polymer matrix. *Materials Technology Reports*, *2*(1), 1603-1603.
[11] Ameh, E. M., Nwogbu, C. C., & Agbo, A. O. (2019). Production of Ceiling Board Using Local Raw Materials. *Advance Journal of Science, Engineering and Technology*, *4*(06), 2330-1744.
[12] Ezenwa, O. N., Obika, E. N., Umembamalu, C., & Nwoye, F. C. (2019). Development of ceiling board using breadfruit seed coat and recycled low density polyethylene. Heliyon, 5(11).
[13] Jeremiah-Lekwuwa, C., Jude Ebieladoh, S., Anthony Emeka, E., Echezona Nnaemeka, O., Onyemazuwa Andrew, A., & Kingsley Chidi, N. (2023). Production and thermo-structural analysis of a hybridized natural fibre-based ceiling board for building applications. *Advances in Mechanical Engineering*, *15*(12), 16878132231216677.
[14] Ikubanni, P. P., Ogunsemi, B. T., Oladimeji, S. O., Adaja, T. A., Enahoro, D. E., Adeleke, A. A., & Aladegboye, O. (2024). Production and physico-mechanical properties of ternary-made (waste ceramics, waste papers, and sawdust) particleboard. In 2024 International Conference on Science, Engineering and Business for Driving Sustainable Development Goals (SEB4SDG) (1-7). IEEE.
[15] Abutu J., Lawal S.A., Ndaliman M.B., Lafia-Araga R.A., Adedipe O. & Choudhury I. A. (2019). Production and Characterization of Brake pad developed from Coconut shell reinforcement material using Central Composite Design. SN Applied Sciences. 1:18.

[16] Abassi, Z., Khoury, E. E., Karram, T., & Aronson, D. (2022). Edema formation in congestive heart failure and the underlying mechanisms. *Frontiers in cardiovascular medicine*, *9*, 933215.
[17] Irechukwu, C. C., Khan, R. H., Abutu, J., Lawal, S. A., & Namessan, N. O. (2021). Effect of tungsten inert gas welding parameters on the performance of AISI 304 alloy steel using multi-response optimisation technique. Welding International, 35(1-3), 45–58.
[18] Mann, G. S., Azum, N., Khan, A., Rub, M. A., Hassan, M. I., Fatima, K., & Asiri, A. M. (2023). Green composites based on animal fibre and their applications for a sustainable future. Polymers, 15(3), 601.
[19] Bergeret, G., & Gallezot, P. (2008). Particle size and dispersion measurements. Handbook of heretogeneous catalysis, 2, 738-765.
[20] Castellanos, A. (2005). The relationship between attractive interparticle forces and bulk behaviour in dry and uncharged fine powders. Advances in physics, 54(4), 263-376.
[21] Kumar, V., Abubakar, A. S., Qureshi, T., Adebanjo, A. U., Kutty, S. R. M., & Abd Razak, S. N. (2025). Sustainable Building Materials from Agricultural Wastes. In Sustainable Green Infrastructure: Materials and Technologies (97-119). Singapore: Springer Nature Singapore.
[22] Hidalgo, D., & Verdugo, F. (2025). Harnessing Secondary Resources for Sustainable and Circular Practices in the Construction Sector: A Scoping Review. Applied Sciences, 15(10), 5410.
[23] Abera, Y. A. (2024). Sustainable building materials: A comprehensive study on eco-friendly alternatives for construction. Composites and Advanced Materials, 33, 26349833241255957.